Soil Dynamics and Earthquake Engineering 124 (2019) 151–161

Contents lists available at ScienceDirect

Soil Dynamics and Earthquake Engineering

journal homepage: www.elsevier.com/locate/soildyn

Influence of fabric anisotropy on seismic response of circular foundation

Jin Qin[a,*], Xiangwu Zeng[b], Haiyan Ming[c]

[a] GZA GeoEnvironmental, Inc., New York, NY, USA
[b] Department of Civil Engineering, Case Western Reserve University, Cleveland, OH, USA
[c] Department of Civil Engineering, Shenzhen University, Shenzhen, China

ARTICLE INFO

Keywords:
Angular sand
Centrifuge modeling
Circular foundation
Fabric anisotropy
Seismic response

ABSTRACT

Earthquake induced foundation failure has occurred in a number of events worldwide, such as the 1964 Niigata earthquake and 1995 Kobe earthquake. Fabric anisotropy has been considered as one of the factors that affect liquefaction characteristics. In this study, dynamic centrifuge tests were conducted for studying the influence of sand fabric anisotropy on seismic response of circular foundations. For this purpose, sub-angular Toyoura sand was used as the most anisotropic material, while sub-rounded Nevada sand was used for the comparison tests. Each group of tests were carried out in both dry and saturated conditions.

These tests are considered complementary to similar centrifuge tests that the authors performed using rectangular foundations. The tests show that sand fabric anisotropy has significant impact on the seismic response of circular foundations as well, especially in saturated conditions. Specifically, as the deposition angle of the sand layer increased, the data show a remarkable decrease in acceleration amplitude concurrently with a considerable decrease of pore pressure ratio and foundation settlement. These effects were more pronounced in the sub-angular Toyoura sand. These effects of increased deposition angle are consistent with the corresponding decrease of bearing capacity and increase of footing settlements in static centrifuge tests from the literature.

1. Introduction

In 2015 alone, magnitude seven and greater earthquakes happened 19 times in the world, including two major ones in Nepal. The April 2015 Nepal earthquake (Gorkha earthquake) killed over 8000 people and injured more than 21,000. Liquefaction is a phenomenon that occurs both in natural and man-made events, in which the strength and stiffness of a soil are significantly reduced. It is typically induced by earthquakes or other rapid loading processes. Foundation failure due to soil liquefaction during earthquakes has been and continues to be a major type of damages.

Soil anisotropy is widely observed in the natural deposited sand. It is determined by particle shape, contact, particle roughness, deposition history and many other more. It affects a few important parameters in soil properties including shear modulus, friction angle and bearing capacity. In previous studies, researchers found that fabric anisotropy of soil grains is an important factor in dynamic soil response as well. Brewer [1] introduced the definition of anisotropy as the property of being directionally dependent, and in most cases, the result of weathering of hard rock or sedimentary solids.

Several researches were conducted using true triaxial tests, nonlinear models and their applications in 1970s. Saada and his colleges at Case Western Reserve University investigated the mechanical behavior of anisotropic materials. They used one-dimensional consolidation of the test specimens in a tri-axial cell to simulate field condition [2]. Oda stated that sands deposited in air or in water show anisotropic shear strength in their triaxial compression tests [3]. In the same year, he showed that the geometrical arrangement of contact surface between the grains could have an important bearing on the mechanical properties of granular materials [4]. Similarly, Arthur and Menzies [5] observed the preferred alignment of particles in disturbed and naturally deposited sands. In 1975, Lade and Duncan [6] systematically evaluated previous designs and theories of triaxial test apparatus and developed cubical triaxial tests so as to study anisotropic behavior of soils.

In 1983, Seed et al. [7] indicated that anisotropy influences strength, bearing capacity and liquefaction resistance of sand. At the same time, a database was generated by Saada at Case Western Reserve University with help from the Institute of Mechanics of the University of Grenoble (France). The database was the result of a joint research project, including 260 tests conducted on the cubic and hollow cylinders. It was discussed at an international workshop held in 1987 and the results published in 1989 [8]. In recent years, Zeng and Ni [9] conducted measurement of shear wave velocities in multiple stress planes of isotropically prepared sand specimens under anisotropic

* Corresponding author.
E-mail address: jxq32@case.edu (J. Qin).

https://doi.org/10.1016/j.soildyn.2019.05.025
Received 1 January 2017; Received in revised form 13 May 2019; Accepted 15 May 2019
Available online 31 May 2019

loading using bender elements.

In 1968, Richard et al. [10] used an elastic half-space to represent elastic foundation media and studied the seismic response of single-story elastic structures situated on this media. It was found that the response of the structure may be increased or decreased when compared to the response of the same structure on rigid foundation. However, the limited availability of real physical data increased the difficulty of research on the seismic response. As an advanced modeling technique, geotechnical centrifuge modeling provides realistic physical data for investigating mechanisms of deformation and failure and for validating analytical and numerical methods. Phillips was the first one to recognize the limitation of elastic theory in the analysis of complex structures and proposed the idea of using centrifugal acceleration to simulate increased gravitational acceleration [10]. Followed by Bucky [11], Rowe [12] and Schofield [13], centrifuge modeling played a more and more important role in geotechnical engineering.

Centrifuge modeling as a powerful tool in physical modeling provides valuable physical data for simulation and validation of designs. Due to its high reliability, less time consuming and cost effectiveness, geotechnical centrifuge modeling has also been extensively used for scale modeling of large-scale nonlinear problem, of which gravity is a primary driving force. It is widely used to test models of geotechnical problems such as the strength, stiffness and capacity of foundations for bridges and buildings. In addition, it is also common to see its application to problems such as settlement of embankments, stability of slopes, earth retaining structures, tunnel stability and seawalls. It is one of the a few methods that models can be subjected to self-weight stress levels with both strain and boundary conditions that are compatible with those existing in a full-scale field structure.

Arulanandan et al. simulated earthquake motions in a centrifuge and used it to study the dynamic response of a clay embankment in a centrifuge in 1982. The results indicated that centrifuge testing could be used to verify analytical techniques used in dynamic studies, as has been for static tests [14]. In the following year, Arulanandan and his colleagues performed dynamic centrifugal model testing to study the generation and dissipation of excess pore water pressures, and to estimate the threshold peak ground acceleration, and the threshold shear strain necessary for the initiation of excess pore water pressure [15]. The dynamic response of a 10.7 m thick dry sand layer was modeled on the Cambridge University centrifuge at scale factors of 35 and 80 by Lambe and Whitman. The results of the tests indicated that a simple sand layer can be effectively modeled abroad a centrifuge and that horizontal accelerations, cyclic shear strains, and settlements follow the scaling laws that govern dynamic centrifugal modeling [16].

Yamaguchi et al. carried out a series of loading tests using Toyoura sand in centrifuge to investigate the scale effect of bearing capacity of dense sand for shallow foundation [17]. Kimura et al. conducted several studies on bearing capacity problems on centrifuge. The researchers demonstrated that similar behavior would be observed as long as the same sand is used in both a centrifuge test and a prototype [18]. Okamura et al. implemented a series of centrifuge model loading tests on dense sand overlying soft clay. They found that the bearing capacity increase with the rising sand thickness-footing width ratio until it reaches that for a infinite sand layer [19].

Liu and Dobry [20] performed centrifuge model experiments to investigate the mechanism of liquefaction-induced settlement of a shallow foundation in 1997. It was found that as the compaction depth increased and approached the total thickness of the soil deposit, the footing acceleration during shaking increased and its settlement decreased. In 2008, Rayhani and El Naggar [21], using centrifuge tests, simulated the behavior of a rectangular building on a 30 m uniform and layered soft soils and a numerical model was developed to simulate the response of two instrumented centrifuge models on soft clay so as to investigate the factors that affect the seismic ground response. Recently, centrifuge tests were introduced to study the effect of fabric anisotropy on seismic response of soil structures. Li [22] found that inherent fabric anisotropy of soil has significant impact on the response of retaining walls and strip foundations in bearing capacity and settlement. Yu [23] discovered that fabric anisotropy also has considerable influence on the liquefaction potential of sand. Qin et al. [24] designed a series of centrifugal tests with different foundation shapes to investigate the effect of fabric anisotropy, including shape factor.

This paper reports the results of two groups of centrifuge tests conducted on models of dry and saturated samples prepared with 0, 45 and 90° deposition angles, respectively. The main objective of these tests is to study the influence of fabric anisotropy on seismic response of circular foundations. The results of parallel studies on influence of fabric anisotropy on seismic responses of rectangular foundations and has been reported by Qin et al. [25].

2. Facilities and instumentation

2.1. Geotechnical centrifuge and control system

A total of twelve tests were conducted on Case Western Reserve University geotechnical centrifuge. The payload capacity of the centrifuge is 20 g-ton with a maximum acceleration of 200 g for static tests and 100 g for dynamic tests. It has a radius of 1.07 m while the dual platforms lie at a radius of 1.37 m.

The centrifuge was constructed in a below ground open and square chamber with a height of 1.8 m and sides of 4.2 m in 1997. It is surrounded by 15 cm thick reinforced concrete walls and support slab. The control room floor level is raised about 1 m above that of the laboratory to provide for additional safety [26].

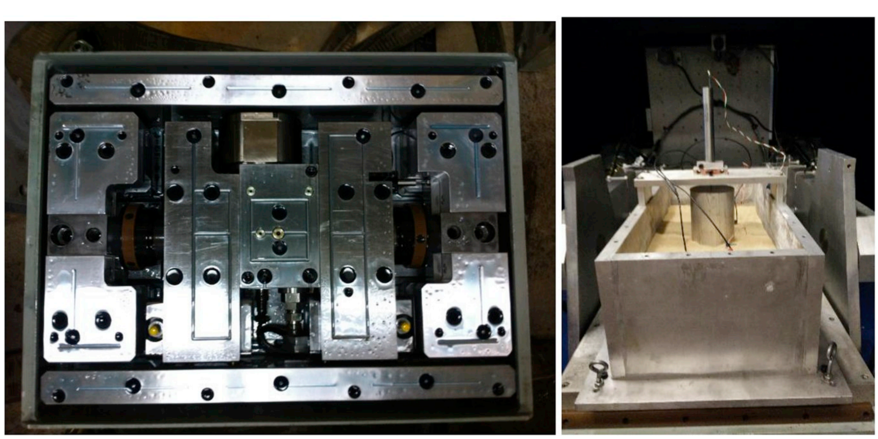

Fig. 1. CWRU electro-hydraulic shaker (L) and test platform (R).

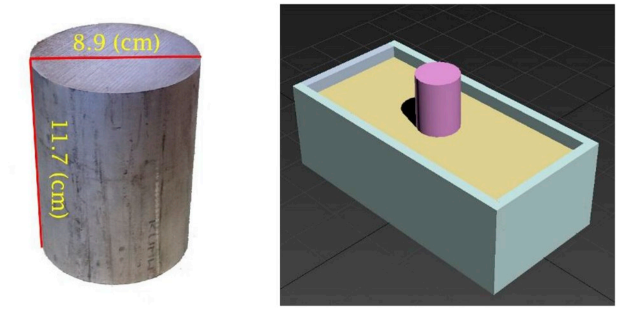

Fig. 2. Scaled model and model container.

Fig. 3. Particles of Nevada (L) and Toyoura (R) under microscope.

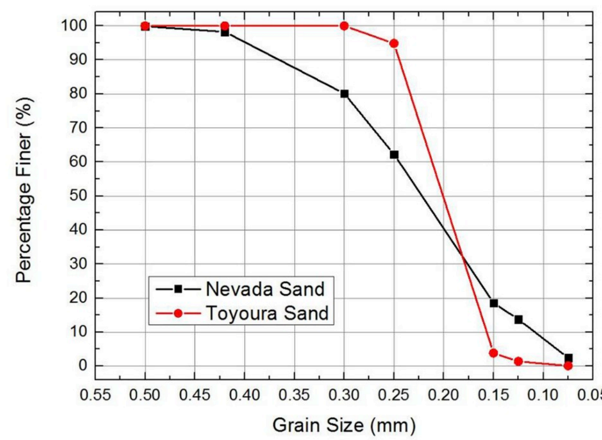

Fig. 4. Particle size distribution Curve of Toyoura and Nevada sand.

Table 1
Properties of Toyoura sand.

Properties	Value	Particle Shape	Value
Mean grain size (mm)	0.20	C_u	1.59
Maximum Density (g/cm^3)	1.332	C_c	0.96
		G_s	2.65
Minimum Density (g/cm^3)	1.646	D_{50}	0.17 mm
		D_{10}	0.16 mm
Internal Friction Angle	34°	e_{max}	0.98
		e_{min}	0.60

2.2. Hydraulic shaker

The electro-hydraulic shaker (Fig. 1) is a high performance servo-mechanism, optimized for high-frequency operation. It can be programmed to achieve the required input motion. The direction of shaking is perpendicular to the vector of rotation of the centrifuge.

A rigid model container was designed and used in experiment. The internal dimensions of the box are 53.3 cm (length) ×24.1 cm (width) ×17.7 cm (height). Unlike laminar container, rigid container cannot accurately represent actual ground response during the test. Nevertheless, it has negligible impact on the results since the tests are aim at the relative changes in response due to fabric anisotropy.

2.3. Instrumentation

Three types of measuring instruments were used in the tests: accelerometers (ACC), pore water pressure transducers (PPT), and linear variable displacement transformers (LVDT). Accelerometers convert the high-impedance charge signal into a useable low-impedance voltage signal to a voltage readout. Similarly, the outputs of PPTs and LVDTs provide real-time data of pressure and displacement during the tests. In addition, a wide range of static and dynamic tests data were collected by the designed data acquisition system. Instrument calibrations were performed prior to the tests and checked again after each test.

3. Model preparation

Centrifuge modeling is a reduced scale version of the prototype and has the necessity of reproducing the soil behavior both in terms of strength and stiffness. In this project, a scaled circular foundation model (Fig. 2) was made of aluminum. It is 11.7 cm in height and 8.9 cm in diameter. The mass of the prototype is 250 tons. The pressure induced by the foundation on the ground was approximate 145 kPa. The model was placed on top of the sand in the container without any fixation. Due to the model size and equipment limitation, the model was place slightly unsymmetrical.

Two types of sands were selected in this study. Toyoura silica sand, as one of the well-known angular materials, has been widely used in studies on soil anisotropy. The designed relative density for the tests in prototype is 65% (e = 0.847) and the average saturated unit weight for the sands is 20 (kN/m^3). Sieve analysis and triaxial tests were performed to study properties of the soils. The permeability coefficient measured for Toyoura sand at this relative density in prototype scale is 1.1×10^{-4} (m/s) (See Table 1). In comparison, a set of tests were repeated by using a sub-rounded sand called Nevada sand also at 65% relative density (e = 0.751). The permeability coefficient for Nevada sand at this relative density in prototype scale is 6.6×10^{-5} (m/s) (See Table 2). The e_{max} and e_{min} used for the tests are 0.98, 0.60 for Toyoura sand and 0.87, 0.53 for Nevada sand.

All models were prepared by using air pluviation method. Chen et al. [27] proposed a relationship between the relative density, drop height and rigid tube diameter. Pre-test measurement were performed to calculate unit weight, void ration and relative density.

Pictures of sand particles under microscope were presented in Fig. 3 and the results of a sieve analysis are shown in Fig. 4.

In preparing the samples, three different deposition angles were introduced so as to make the particles in the models with a predominant direction of orientation. In order to achieve a relative density of 65%, the air pluviation method was selected for the sand pouring process.

Table 2
Properties of Nevada sand.

Source	G_s	e_{min}	e_{max}	γ_d, min (kN/m^3)	γ_d, max (kN/m^3)
Arulmoli et al. (1992) [28]	2.67	0.51	0.887	13.87	17.33
Balakrishnan (1997) [29]	–	0.55	0.84	14.21	16.92
Kammerer et al. (2000) [30]	2.67	0.533	0.887	13.87	17.09

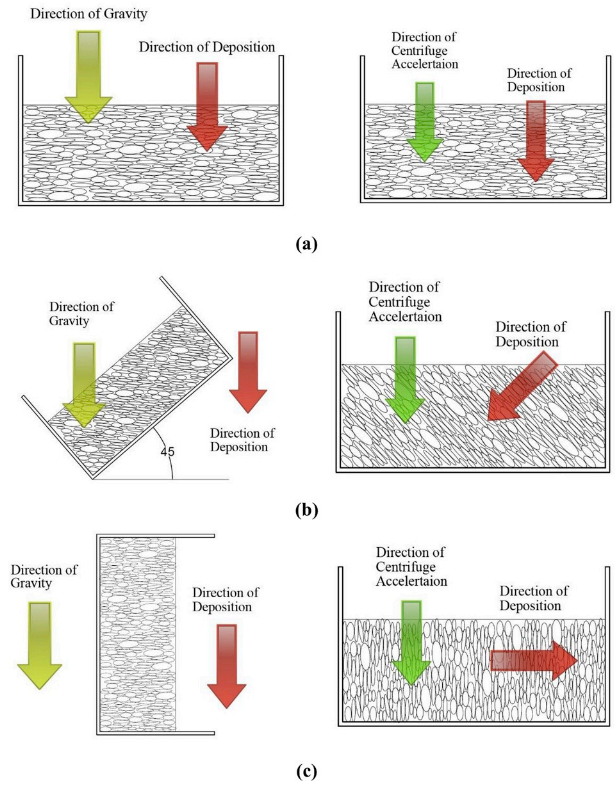

Fig. 5. (a) Model preparation with 0 degree deposition Angle(b) model preparation with 45 degree deposition Angle(c) model preparation with 90 degree deposition angle.

The apparatus consisted of a plastic conical hopper connected to a 20 cm long rigid tube. The density was controlled by the height and rate of pouring. Calibration tests were performed in advance for verification purpose to achieve the designed relative density.

For the model with 0° deposition angle, the rigid container was placed flat on the ground and sand was poured in layers and the instrumentation was installed at the designed locations, which were determined before the tests.

In saturated tests, the pore fluid used in the model test is important for maintaining the correct drainage and effective stress conditions. Deaired water is selected in this study. The model tests are not a replication of a specific prototype structure. Therefore, using water as pore fluid will not significantly change the data interpretation. In some cases, a scaled viscous fluid will be needed to ensure the same scaling factor for dynamic event and pore pressure dissipation.

In terms of 45 and 90° deposition angle tests, the container were titled by 45 or 90° against the wall at first. The end wall of the container was removed to make it easier for pouring. Blocks of Styrofoam were introduced during the pouring to hold the existing sand as its surface rose. Pouring were stopped to install instruments when it reached the appropriate depth. When pouring completed, the end wall was put back and sealed. Container was carefully tilted back to horizontal orientation and all Styrofoam blocks were removed. A leveling device was used to keep sand surface flat and extra sand was removed. The remaining dry sand was weighted to obtain the total weight of sand used so as to calculate the achieved relative density. A sketch of the process for the preparation of centrifuge models is illustrated in Fig. 5.

For saturated tests, a high degree of saturation provides better accuracy for the results. Therefore, after model was constructed, the model container was placed in a wooden saturation box with airtight cover and sealed top. Valves were opened to replace the air in the soil by carbon-dioxide which dissolves easily in water. Then, all valves were closed and de-aired fluid slowly flowed into the soil from the bottom. In

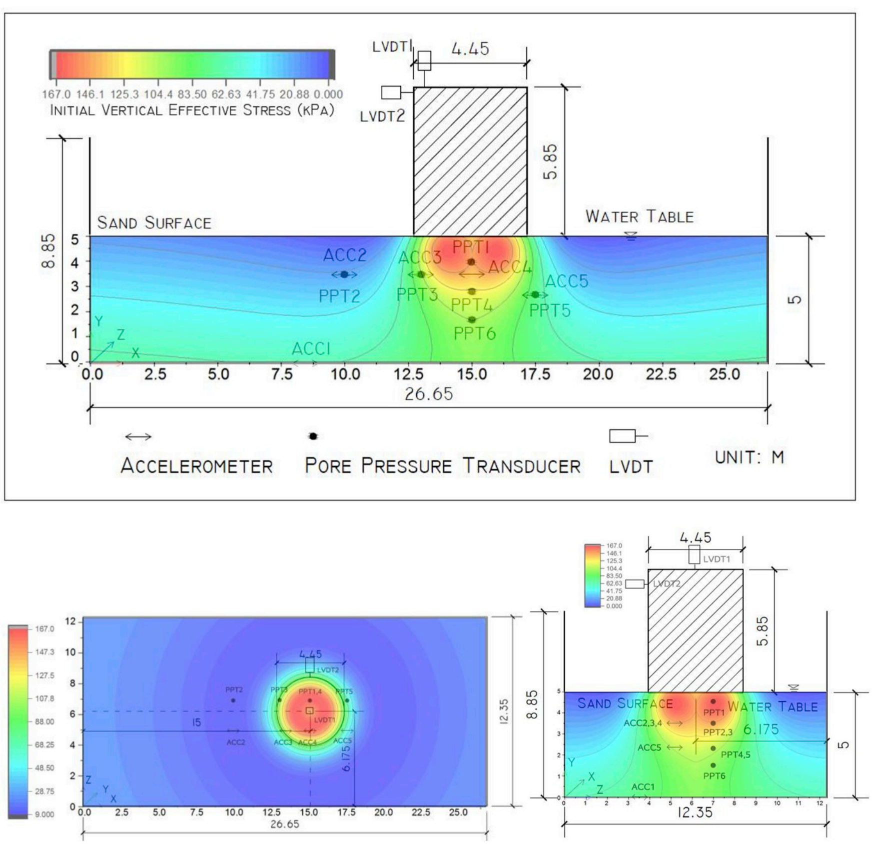

Fig. 6. Cross-sectional view of the centrifuge model.

Table 3
Transducers coordinates system (0 degree, Toyoura, saturated, prototype scale).

Transducers	Design Location of Transducers		
Name	X (m) ± 0.05	Y (m) ± 0.05	Z (m) ± 0.05
ACC1	–	–	–
ACC2	10.0	3.5	5
ACC3	13	3.5	5
ACC4	15	3.5	5
ACC5	17.5	2.5	5
PPT1	15	4.5	7
PPT2	10	3.5	7
PPT3	13	3.5	7
PPT4	15	2.5	7
PPT5	17.5	2.5	7
PPT6	15	1.5	7
LVDT1	–	–	–
LVDT2	–	–	–

addition, vacuum was applied for at least 24 h to obtain a higher degree of saturation.

Three section views of the initial effective stress distribution are shown in Fig. 6, including front view, side view and plan view. The initial vertical effective stresses were calculated by using 3D analysis method. The results were only used for estimating the initial vertical effective stresses for normalizing the pore pressure measurements. Each section was selected at the plane where the largest stress was observed. The soil underneath the foundation experienced higher stress than those in the free field. A maximum value of 153.8 kPa was shown at about half meter below the bottom of the foundation.

4. Test procedures

The profile of each model was measured so that the cross-sectional view of the model before the test can be compared to that after the application of the earthquake motion. Photos of the models were taken at this stage.

After the saturation process was finished, the rigid box was carefully moved from the saturation box and fixed by bolts on one side of the platforms. The counter weight was added to the opposite side of the swing arm. All the transducers were properly connected. Before starting the centrifuge, a complete checkup of all equipment and connections on the arm was carried out.

The centrifuge was then spun up to 50 g gradually and maintained at that speed for 5 min. It ensured that the static excess pore water pressure was dissipated. The input motion was applied. Data were collected from all the transducers through data acquisition system and saved on a computer for analysis. Then, the centrifuge was spun down and post-test measurements were performed. The final locations of the transducers were also measured.

5. Results and discussions

All the data are presented in prototype scale. The transducers locations were determined before the tests and re-measured after the tests. And the locations were maintained the same in all tests for comparison purpose.

The accelerometers are placed in the prototype-horizontal direction to record the horizontal acceleration of the soil at the select depths and the pore pressure transducers are placed in the prototype-vertical direction at the selected depths to investigate when and where liquefaction occurs. In addition, two LVDTs were fixed at the top of the model structure to monitor the horizontal and vertical displacements during the tests.

A sketch of the model is illustrated in Fig. 6. The coordinates of all transducers in one test are shown in Table 3.

5.1. Effect of fabric anisotropy on acceleration

Five accelerometers were used for the tests. One was placed on the shake table to measure the input motion. Three were located in active zone, transition zone and passive zone of general bearing capacity failure pattern, and one more accelerometer was located at the other side of soil with deeper depth for comparison.

A calibration test was performed on the box before conducting the tests so as to simulate the earthquake that would have the desired amplitude and frequency. A comparison of time histories of acceleration record between the achieved input motion and desired input motion was presented in Fig. 7(a). Response spectrum analysis was performed on the representative signals. A comparison in spectral acceleration was also shown in Fig. 7(b). The motions show high similarity both in amplitudes and frequency except for some small spikes. These are likely due to the noise during signal capture and have little to no effect on the tests. Butterworth filter was applied for data analysis and there is no considerable difference noticed for the achieved motions from test to test.

The time histories of acceleration are shown for illustration. Figs. 8 and 9 show two groups of test results recorded by accelerometers (ACC2 and ACC4). ACC4 was installed beneath the foundation with a depth of 1.5 m and ACC2 was place at the same depth in the passive zone.

Comparing Fig. 8 (a) (b) and 9 (a) (b), for the dry tests, amplitudes and time history in acceleration for the models with different deposition angles are similar, except that the difference in maximum amplitudes between tests with 0, 45 and 90° deposition angles with Toyoura sand

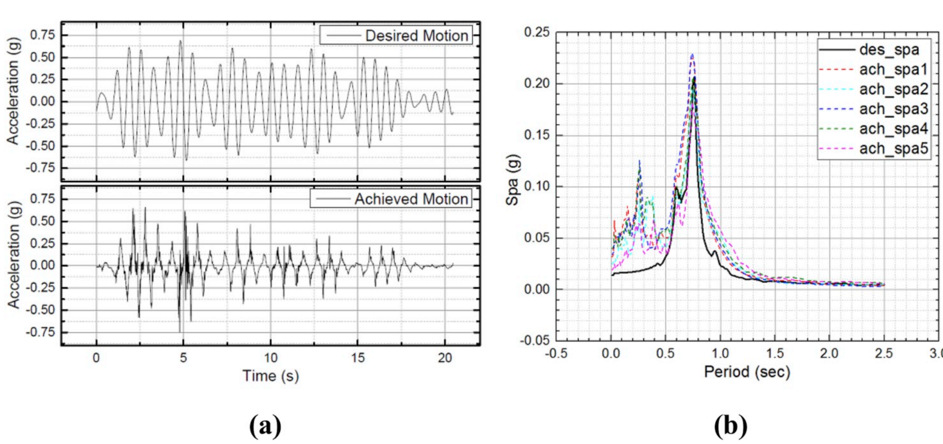

Fig. 7. (a) Comparison between achieved motion and design motion in time History. (b) comparison between achieved motion and design motion in spectral acceleration.

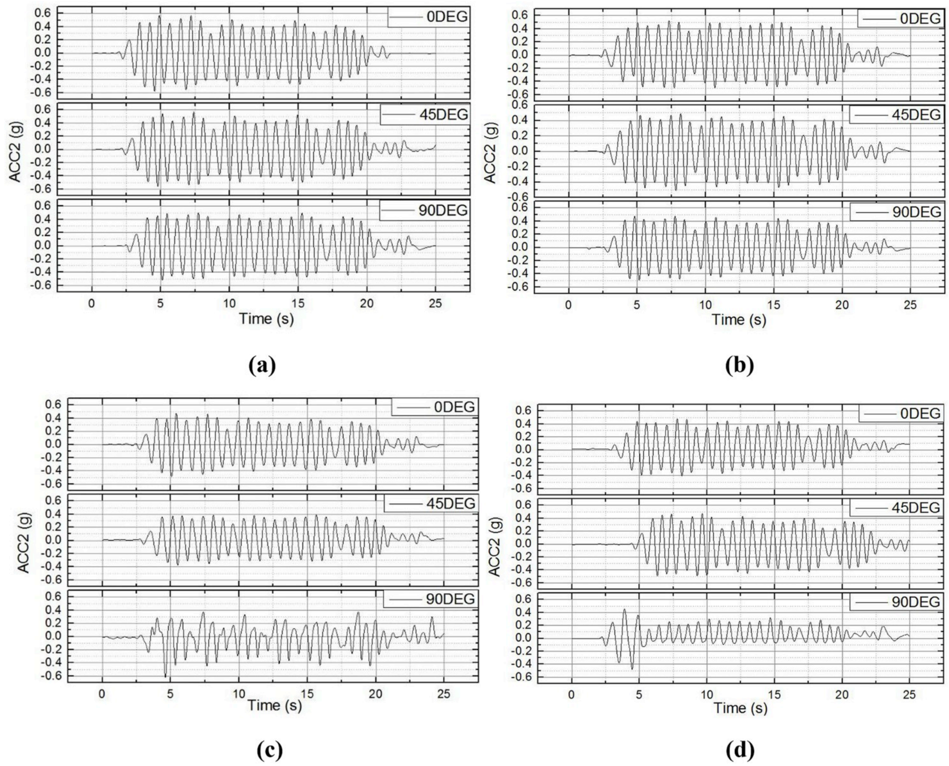

Fig. 8. Time histories of acceleration recorded by ACC2. (a) Toyoura sand, dry (b) Nevada sand, Dry(c) Toyoura sand, saturated (d) Nevada S and, saturated.

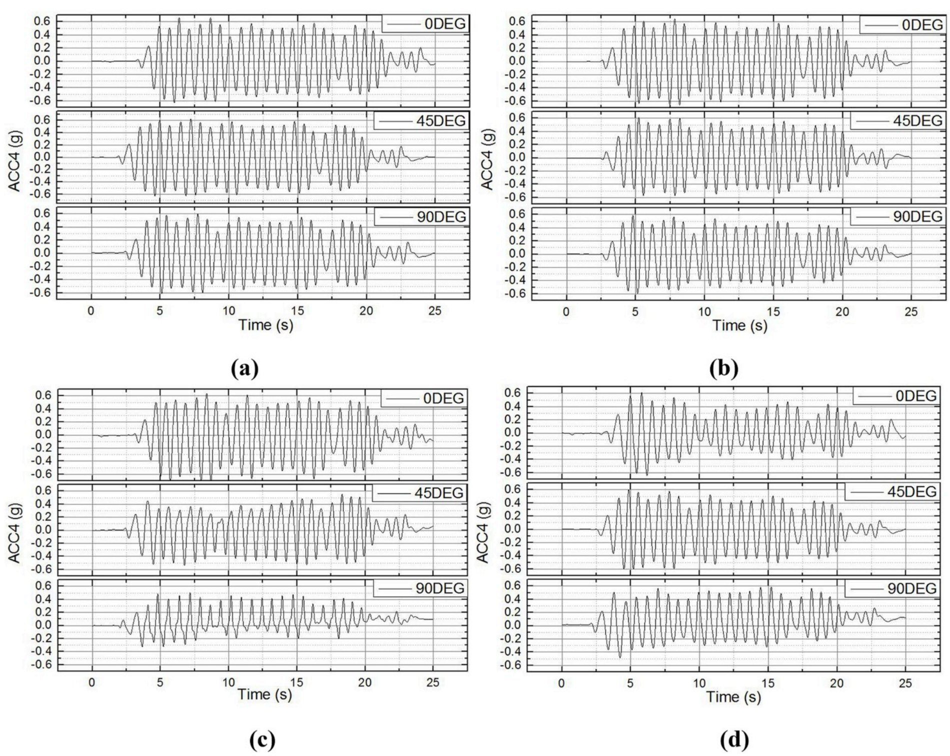

Fig. 9. Time histories of acceleration recorded by ACC4. (a) Toyoura sand, dry (b) Nevada sand, Dry(c) Toyoura sand, saturated (d) Nevada sand, saturated.

are slightly greater than the tests using Nevada sand. For example, for ACC2, the maximum acceleration amplitudes are 0.569, 0.567 and 0.504 g for experiments prepared with 0, 45 and 90° deposition angle using Toyoura Sand, while maximum acceleration amplitudes of 0.522, 0.489 and 0.478 g were recorded for tests using Nevada sand.

On the other hand, for saturated tests, the difference can be easily noticed in the accelerations recorded based on deposition angles, particularly when using Toyoura sand. In Fig. 8 (c)(d) and 9 (c)(d), significant decrease in acceleration amplitudes are shown between 0° test and 45, 90° tests. For instance, the amplitude recorded by ACC4 dropped by as much as 20%. At the same time, in the group of tests with Nevada sand, amplitude reduction can also be noticed, but was much

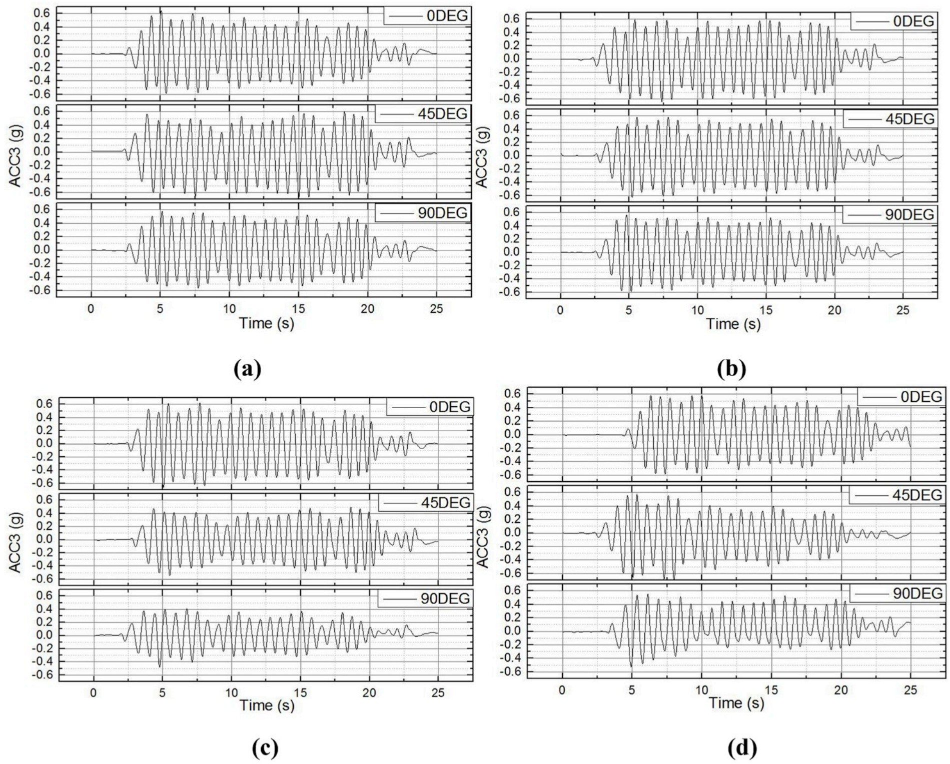

Fig. 10. Time histories of acceleration recorded by ACC3. (a) Toyoura sand, dry (b) Nevada sand, Dry(c) Toyoura sand, saturated (d) Nevada sand, saturated.

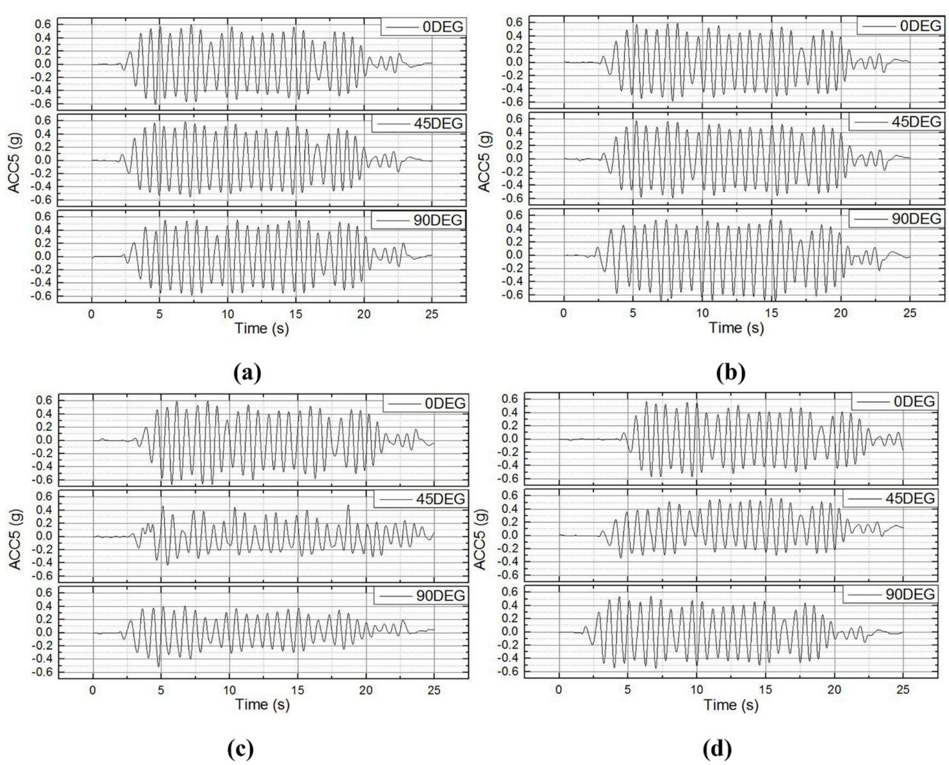

Fig. 11. Time histories of acceleration recorded by ACC5(a) Toyoura sand, dry (b) Nevada sand, Dry(c) Toyoura sand, saturated (d) Nevada sand, saturated.

less significant. Similar trends were also recorded by ACC3 and ACC5 as shown in Figs. 10 and 11.

In general, the smallest amplitude reduction among the tests were recorded in the models deposited by 0° angle. Therefore, it was a higher liquefaction resistance under earthquake loading. Looking at the amplitude recorded and reduction rate, the effect of fabric anisotropy on acceleration in or near the passive earth pressure zone (ACC2) is more significant than that in the active earth pressure zone (ACC4).

5.2. Effect of fabric anisotropy on pore water pressure

In the saturated tests, measurements of excess pore water pressure

Table 4
The initial vertical effective stress.

Transducers	Vertical Effective Stress
Name	Unit (kPa)
PPT1	153.80
PPT2	18.45
PPT3	72.45
PPT4	79.15
PPT5	48.4
PPT6	60.5

ratio directly reflect whether liquefaction happened or not (the ratio is equal to 1 when the soil is liquefied). In this case, liquefaction potential varies at different locations. Places with larger initial effective stress normally result in lower liquefaction potential. In the previous paragraph, a graphic display of the initial vertical effective stress distribution was shown in Fig. 6. (see Table 4). A filter program was adopted for noise reduction purpose. Maximum excess pores pressure are compared in Figs. 12 and 13.

PPT 1, 4 and 6 were placed beneath the model foundation with depth of 0.5, 2.5 and 3.5 m, respectively. PPT2 and PPT3 were located in the passive and transaction zone at the depth of 1.5 m. One last transducer (PPT5) was buried at the opposite side of the model with a deeper location than PPT3.

Only one of the transducers (PPT2) showed sign of liquefaction during the tests (Figs. 12 and 13). Pore water pressure ratio reached 1.00 in all the tests. PPT2 was the farthest sensor from the center of foundation. Hence, it represents the area that has relatively low initial effective stress or so called free field.

PPT3 and PPT5 were under the edge of the model foundation with equal distance away from the foundation. In each group of three tests, the one prepared with 90° deposition angle always has higher value of pore pressure ratio than others. Difference can be recognized more easily in the tests using Toyoura sand. There are about 17% and 22% increase in the ratio from 0° test to 90° test respectively base on the recordings of PPT3 and PPT5.

PPT1, 4 and 6 were lined up vertically in the central axis of the tests. In term of PPT1, soil in this area usually had large vertical stress due to the superstructure. By adding soil vertical stress, the value of initial effective stress become greater. Thus, excess pore pressure ratio was kept low. The values are ranging from 0.158 to 0.164, which means there is little chance that liquefaction will happen. As depth goes

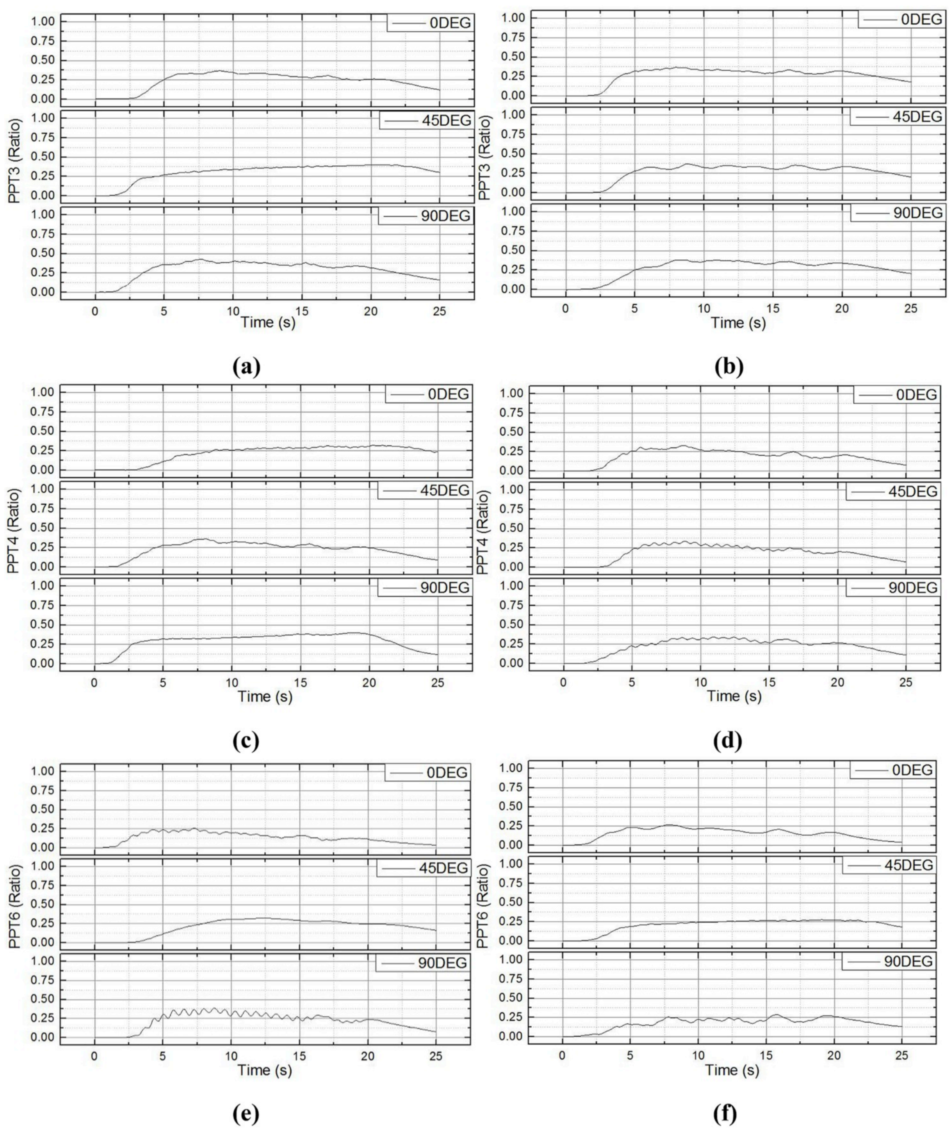

Fig. 12. Time histories recorded by pore pressure transducers. (a) Toyoura, saturated condition (PPT3) (b) Nevada, saturated condition (PPT3)(c) Toyoura, saturated condition (PPT4) (d) Nevada, saturated condition (PPT4)(e) Toyoura, saturated condition (PPT6) (f) Nevada, saturated condition (PPT6).

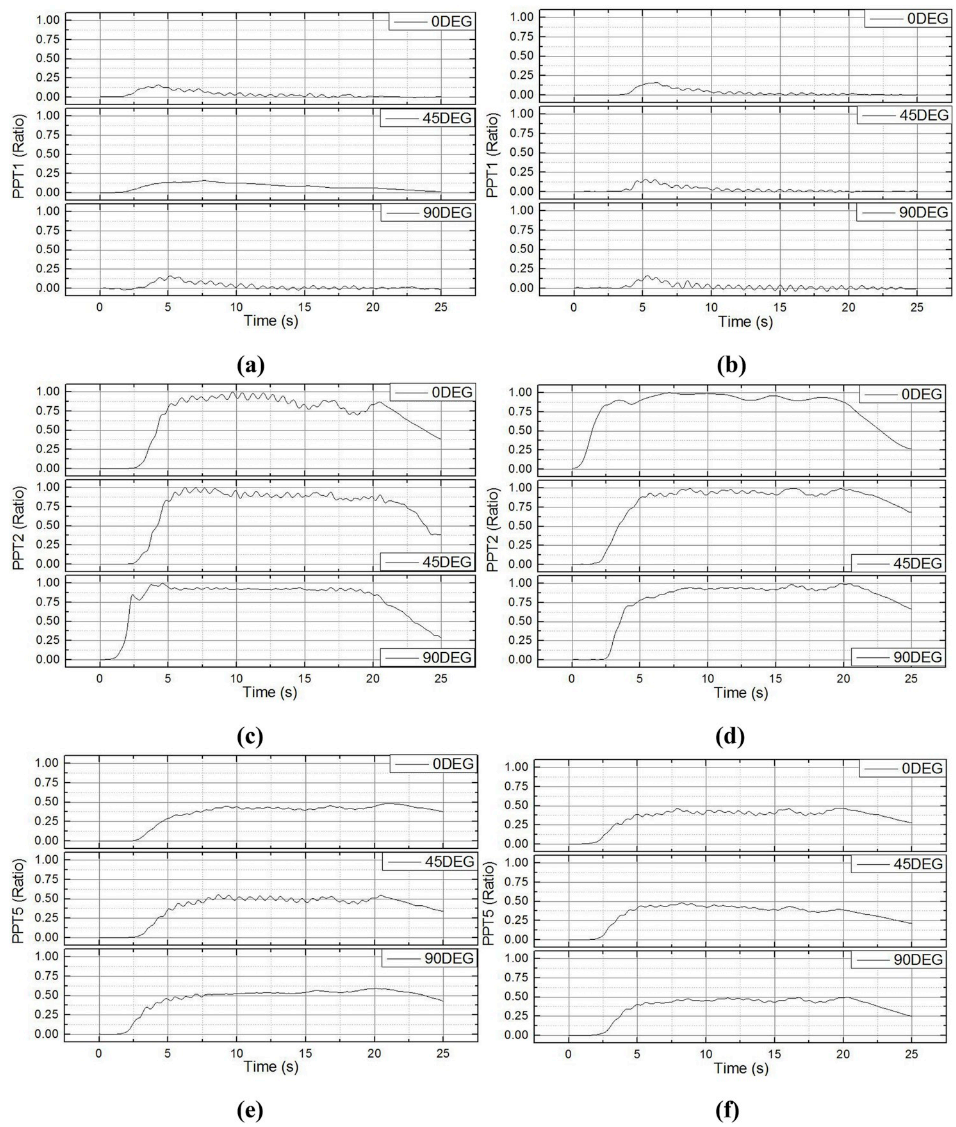

Fig. 13. Time histories recorded by pore pressure Transducers. (a) Toyoura, S aturated condition (PPT1) (b) Nevada, saturated condition (PPT1)(c) Toyoura, saturated condition (PPT2) (d) Nevada, saturated condition (PPT2)(e) Toyoura, saturated condition (PPT5) (f) Nevada, saturated condition (PPT5).

deeper, value of excess pore pressure ratio increases, which indicates that location depth did play an important role in determining its liquefaction potential.

Above all, fabric anisotropy can be seen from most of transducers records. And for each location, the difference between the tests of each group were more obvious when Toyoura sand was used.

5.3. Effect of fabric anisotropy on displacement of the building

Time histories of displacements in dry condition tests were shown in Fig. 14. LVDT1 measured settlements and LVDT2 measured horizontal displacements. In Fig. 14 (c) and (d), 0.8 cm was measured for both 0° deposition angle tests using Toyoura and Nevada sand. When it come to the tests prepared by 90° deposition angle, the readings increased to 1.21 and 1.80 respectively. Similar trend can be found on settlements. Though the difference is not significant, the effect of fabric anisotropy can still be detected even in the dry tests (see Table 4).

Nevertheless, there were very substantial settlements observed in saturated tests. All of the readings excessed the measurement range of the LVDTs. Instead, they were measured and recorded manually and are shown in Table 5. The total prototype foundation settlements measured in the tests are in the range between 14.6 and 36.0 cm, corresponding to a settlement/diameter ratio S/D = 3.28–9.80%. For Nevada sand tests, the settlement of the foundation increases as the deposition angle increases. For Toyoura tests, the value of the settlement of 90° test are more than twice that in 0° test. Therefore, it is obvious that fabric anisotropy has significant impact on displacements. In all test, model prepared by 90° deposition angle settled more than others.

Tilting was observed during the tests, particularly in saturated tests. Its direction varies from test to test. Rocking was rarely observed in the circular footing tests. It was seen often in the tests using rectangular footing. The distance between center of gravity and pivot of circular footing (4.45 cm) is far greater than that of rectangular footing (1.9 cm). Self-weight plays important roles by preventing the structure from rocking or tilting.

6. Conclusions

Series of centrifuge tests were conducted to investigate the influence of fabric anisotropy on the seismic response of circular foundations. Based on the results of the tests, the following conclusions can be drawn:

1) Effect of fabric anisotropy was less significant under dry condition

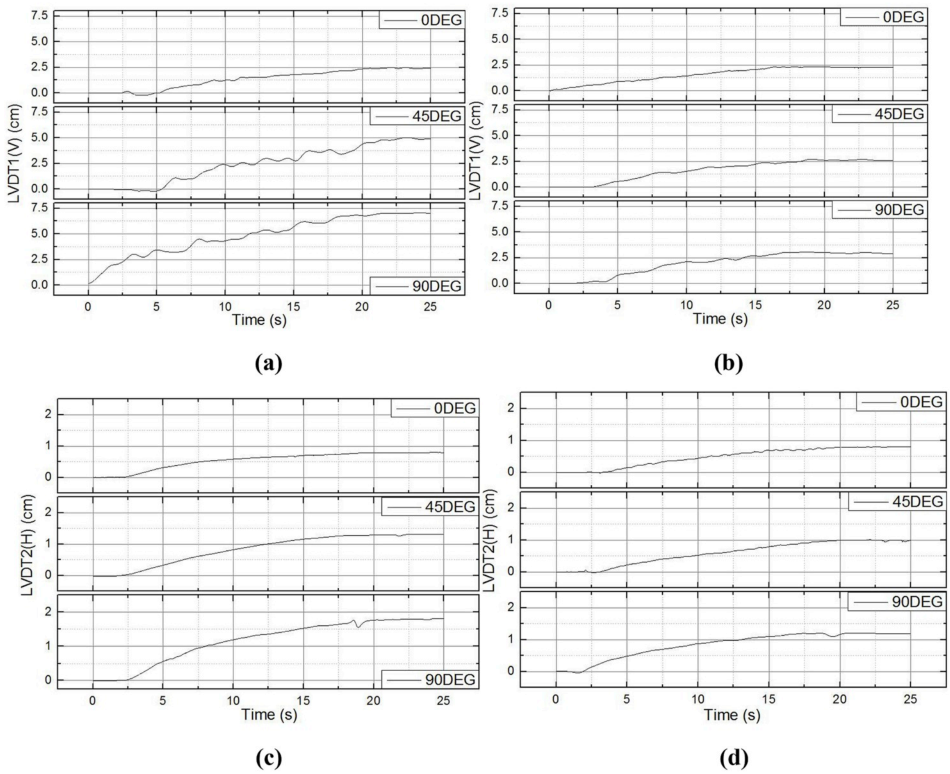

Fig. 14. Time histories recorded by LVDTs in dry condition. (a) Toyoura S and, vertical displacement (b) Nevada S and, vertical Displacement. (c) Toyoura S and, horizontal displacement (d) Nevada S and, horizontal displacement.

Table 5
Test results of settlements.

Sample	Toyoura Sand						Nevada Sand					
Conditions	Dry			Saturated			Dry			Saturated		
Deposition Angle	0	45	90	0	45	90	0	45	90	0	45	90
LVDT1 (V)(cm)	2.49	5.02	7.08	14.6	20.1	36.0	2.34	2.71	3.07	16.7	18.2	19.8
LVDT2 (H)(cm)	0.80	1.31	1.81	–	–	–	0.80	1.00	1.21	–	–	–

than under saturated condition. This effect was more pronounced in passive zone than in active zone. The models prepared with 0 deposition angle has the most liquefaction resistance. This coincides with the findings of the tests using rectangular foundation.

2) Fabric anisotropy has strong effect on excess pore pressure during seismic motion. The pore pressure ratio under the foundation are smaller than those in the free field. Surcharges may help reduce the excess pore pressure and the magnitude of settlements.
3) Deposition angle has large impact on displacements. The magnitude of displacements increased significantly with deposition angle used in model preparation. This agrees with the results of rectangular foundation tests. It is shown that effect of fabric anisotropy on displacements is more significant with the existence of water.
4) Effect of fabric anisotropy is more pronounced in the angular Toyoura Sand even though in the sub-rounded Nevada Sand the deposition angle still has some influence in the seismic response of the model. Sands with angular shape like Toyoura sand have a strong fabric anisotropy, which should be considered as an important parameter in engineering design.
5) Foundation shape does not have major impact on seismic response of foundation. The recordings in each group have identical trends.

Acknowledgments

The authors would like to thank the partial support by National Natural Science Foundation of China under Grant No. 51278307.

References

[1] Brewer R. Fabric and mineral analysis of soils. 1964.
[2] Saada AS. One-diemensional consolidation in triaxial cell. J Soil Mech Found Div 1970;96(3):1085–9.
[3] Oda M. Initial fabrics and their relations to mechanical properties of granular material. Soils Found 1972;12(1):17–36.
[4] Oda M. The mechanism of fabric changes during compressional deformation of sand. Soils Found 1972;12(2):1–18.
[5] Arthur J, Menzies B. Inherent anisotropy in a sand. Geotechnique 1972;22(1):115–28.
[6] Lade PV, Duncan JM. Cubical triaxial tests on cohesionless soil. J Geotech Geoenviron Eng 1975:101. ASCE# 11269 Proceeding.
[7] Seed HB, Idriss I, Arango I. Evaluation of liquefaction potential using field performance data. Journal of Geotechnical Engineering 1983;109(3):458–82.
[8] Saada AS. State-of-the-art paper: hollow cylinder torsional devices: their advantages and limitations. Advanced triaxial testing of soil and rock. ASTM International; 1988.
[9] Zeng X, Ni B. Stress-induced anisotropic G max of sands and its measurement. J Geotech Geoenviron Eng 1999;125(9):741–9.
[10] Phillips E. De l'equilibre des solides elastiques semblables. CR Academy of Science. Paris 1869;68:75–9.
[11] Bucky PB. Use of models for the study of mining problems. Incorporated: American Institute of Mining and Metallurgical Engineers; 1931.
[12] Rowe P, Craig W. Prediction of caisson and pier performance by dynamically loaded

centrifuge models. Symp. On Foundation Aspects of Coastal Structures; 1978.
[13] Schofield AN. Cambridge geotechnical centrifuge operations. Geotechnique 1980;30(3):227–68.
[14] Arulanandan K, Canclini J, Anandarajah A. Simulation of earthquake motions in the centrifuge: J geotech engng div ASCE, V108, NGT5, may 1982, P730–742. International journal of rock Mechanics and mining sciences & geomechanics abstracts. Pergamon; 1982.
[15] Arulanandan K, Anandarajah A, Abghari A. Centrifugal modeling of soil liquefaction susceptibility. Journal of Geotechnical Engineering 1983;109(3):281–300.
[16] Lambe PC, Whitman RV. Dynamic centrifugal modeling of a horizontal dry sand layer. Journal of Geotechnical Engineering 1985;111(3):265–87.
[17] Yamaguchi H, Kimura T, Fuji N. On the influence of progressive failure on the bearing capacity of shallow foundations in dense sand. Soils Found 1976;16(4):11–22.
[18] Kimura T, Kusakabe O, Saitoh K. Geotechnical model tests of bearing capacity problems in a centrifuge. Geotechnique 1985;35(1):33–45.
[19] Okamura M, Takemura J, Kimura T. Centrifuge model tests on bearing capacity and deformation of sand layer overlying clay. Soils Found 1997;37(1):73–88.
[20] Liu L, Dobry R. Seismic response of shallow foundation on liquefiable sand. J Geotech Geoenviron Eng 1997;123(6):557–67.
[21] Rayhani M, El Naggar MH. Numerical modeling of seismic response of rigid foundation on soft soil. Int J Geomech 2008;8(6):336–46.
[22] Li B, Zeng X, Ming H. Seismic response of retaining wall with anisotropic backfills. Earth retention conference. vol. 3. ASCE; 2010.
[23] Yu H, et al. Effect of fabric anisotropy on liquefaction of sand. J Geotech Geoenviron Eng 2012;139(5):765–74.
[24] Qin J, Zeng X, Ming H. Influence of fabric anisotropy on seismic responses of foundations. Journal of Rock Mechanics and Geotechnical Engineering 2015;7(2):147–54.
[25] Qin J, Zeng X, Ming H. Centrifuge modeling and the influence of fabric anisotropy on seismic response of foundations. J Geotech Geoenviron Eng 2015;142(3):04015082.
[26] Figueroa J, et al. Development of the geotechnical centrifuge at case western Reserve university. Proceedings of the international conference: centrifuge. 1998.
[27] Chen H-T, Lee C-J, Chen H-W. The traveling pluviation appartus for sand specimen preparation. Proceedings of the international conference centrifuge. 1998.
[28] Arulmoli K. VELACS: verification of liquefaction analyses by centrifuge studies, laboratory testing program. Soil data report; 1992.
[29] Balakrishnan A, Kutter B, Idriss I. 'Liquefaction remediation at bridge sites—centrifuge data report for BAM05. Rep. No. UCD/CGMDR- 1997;97:10.
[30] Kammerer A, et al. Cyclic simple shear testing of Nevada sand for PEER Center project 2051999. Geotechnical Engineering Research Report UCB/GT/00-01. Berkeley, Calif: University of California; 2000.